# Photoelectric effects in magnesium aluminum spinel

J. D. Woosley and C. Wood
*Northern Illinois University, DeKalb, Illinois 60115*

E. Sonder and R. A. Weeks
*Oak Ridge National Laboratory, Oak Ridge, Tennessee 37830*

(Received 2 November 1979)

The electronic and transport properties of magnesium aluminum spinel have been investigated photoelectrically. Photoemission of holes and electrons into spinel from metal contacts (Pt, Au, Ta, Mo, and Cu) has been used to determine barrier heights. From this information, as well as vacuum-uv photoconductivity data, we have obtained the following energy-band parameters: The Fermi level lies $\sim 3$ eV below the bottom of the conduction band, which in turn is located $\sim 2$ eV below the vacuum level, and the band gap is $\sim 9$ eV. Photoemission was not observed from graphite electrodes which form Ohmic contacts. Electron, neutron, or gamma irradiation produced three photoconductivity bands of half-width $\sim 0.5$ eV, with peaks at 4.5, 5.0, and 5.5 eV. The three bands, equally spaced in energy, may be associated with the same center. The optical absorption band of the $F$ center is in the same region of the spectrum; however, its shape did not correspond to the observed photoconductivity spectrum. A lower limit of $10^{-6}$ $cm^2/V$ has been calculated for the $\mu\tau$ product of the photogenerated charge carriers.

## I. INTRODUCTION

Photoconductivity in insulators such as alkali halides[1-3] and MgO (Refs. 4 and 5) has been associated with optically absorbing defect centers. A major object of this research was to relate the photoconductivity spectrum in magnesium aluminum spinel to the optical absorption. No such relation was found, but in the course of this work it was found that many of the photoresponse peaks originally attributed to photoconductivity were actually due to photoemission at the metal-insulator contact. Barrier heights for a metal-insulator junction can be determined by observing photoemission from the metal into the insulator and have been reported for $SiO_2$, $Al_2O_3$, and alkali halides.[6,7] Under proper experimental conditions, these measurements can be used to determine the band gap of the insulator. In this paper clear distinction is made between photoemission and photoconductivity in magnesium aluminum spinel, and some band structure and photoconductivity parameters were obtained from these photoelectric measurements.

## II. EXPERIMENTAL

### A. Source and purity of material

Nominally pure ⟨111⟩ spinel crystal disks were obtained from the Single Crystal Products Division, Union Carbide Corporation. Samples doped with 200 ppm Fe were obtained from the same source. Nonstoichiometric spinel samples were provided by Hickmott at Wright-Patterson AFB.

### B. Sample preparation

Samples were cut to size with a diamond saw, ground, and polished with 1 $\mu$m $Al_2O_3$ abrasive. Two sample configurations were used and they are depicted in Fig. 1. Electrodes were sputtered onto the large faces. Electrode materials were Pt, Au, Cu, Mo, Ta, and graphite, and various thicknesses were deposited. In the usual configuration,

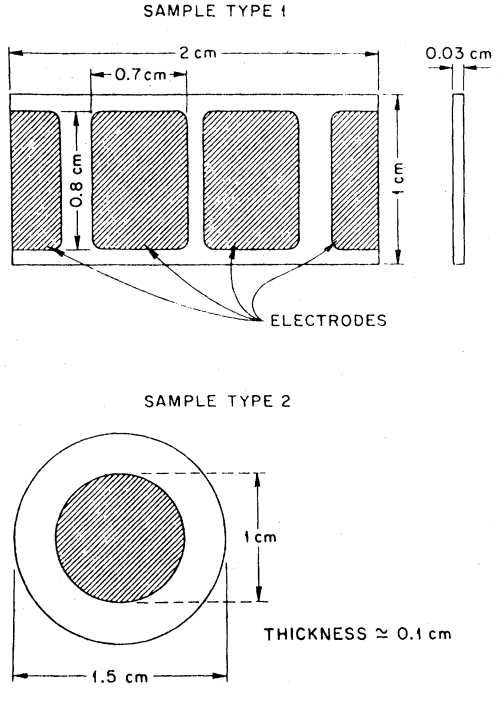


FIG. 1. Sample and electrode configurations.

 

semitransparent electrodes ~100 Å thick were deposited on one side, and opaque ones, ~0.5 μm thick on the opposite side. Ag wires with a 0.005-in. diameter, were attached to the electrodes with conductive silver paint.

### C. Experimental arrangement

Illumination was provided by a Bausch and Lomb high-intensity grating monochromator and lamp with adjustable slits. Dispersion was a constant 33 Å/mm. During photoemission measurements, the slit width was set at 3.00 mm. This resulted in a bandwidth of 100 Å, corresponding to an energy range of 0.2 eV at 5.0 eV, which increased as the square of the photon energy. For photoconductivity measurements, the slit width was decreased to 0.75 mm. Corresponding figures for bandwidth and energy range are 25 Å and 0.05 eV, respectively, at 5.0 eV.

Two xenon lamps were used to provide illumination over the range 0.75 to 6.2 eV. A 100-W Bausch and Lomb lamp was used for photoconductivity measurements and a 250-W model, manufactured by Schoeffel Instrument Company, was used for photoemission measurements. Both lamps, when checked with a photodiode, were stable to within ±5%. Quantitative flux measurements were made with an Eppley Thermopile and Microvolt Comparator. Absolute accuracy of these flux measurements was estimated to be ±5% in the range of 1.5 to 4.0 eV, ±10% from 4.0 to 5.0 eV, and ±20% for energies greater than 5.0 eV.

A schematic of the apparatus is depicted in Fig. 2. The monochromator output passed through a fused-quartz plate into a vacuum chamber. The sample was mounted inside, perpendicular to the beam, about 8 cm from the monochromator exit slit. This distance provided enough beam dispersion to ensure that the sample was uniformly illuminated. The intensity was high enough to ensure a strong signal.

For the measurements, a dc electric field was applied across the sample with either dry-cell batteries or a Keithley 240 A HV supply. The sample was illuminated and the resulting current measured with an electrometer. Four different electrometers, Keithley models 610C, 610R, 615, and 616, were used, but the majority of measurements were made with the 610C. Noise level varied from $10^{-13}$ to $10^{-16}$ A depending on the electrometer.

Measurements were made from long to short wavelength. The sample was shuttered to light between measurements. The monochromator was set for the desired wavelength with the shutter in place. The shutter was lifted and the sample illuminated until its photocurrent was at maximum. This value was then recorded, and the shutter closed while the photocurrent decayed. The process was then repeated at a different wavelength setting.

When dark currents were large relative to the total light current, the dark current was measured prior to exposure and subtracted from all readings. The corrected values were then recorded as the photocurrent. If the dark current was $\leq 1\%$ of the total light current, the measured value was recorded directly as photocurrent.

### D. Classification of the photocurrent

An observed photocurrent may be produced by photoconductivity, photoemission from the con-

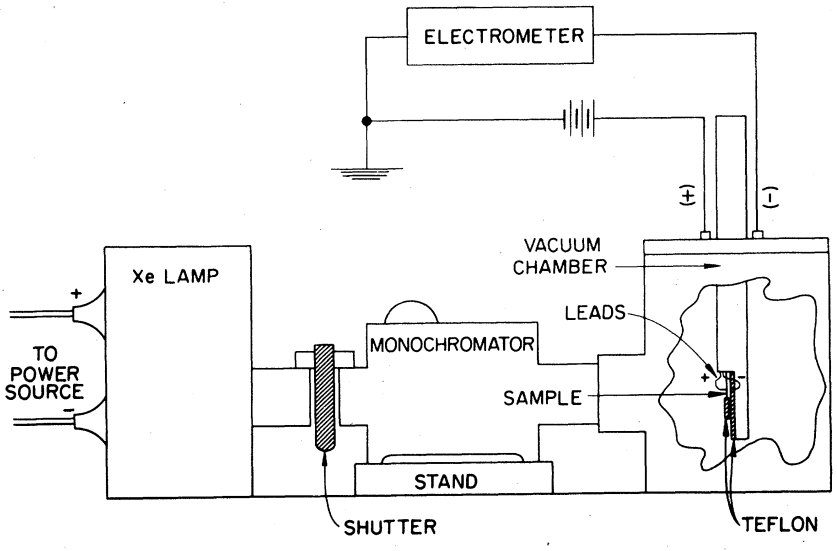


FIG. 2. A schematic of the experimental apparatus.

tacts, or photoemission from surface states of the sample.[8] The configuration of our sample electrodes permitted these three effects to be separately determined by the following procedure. The sample was mounted with the thin, semitransparent electrode illuminated, and a photoresponse versus incident photon energy measurement was taken with the thin electrode at a positive dc potential relative to ground. Then the applied potential was reversed and a second photoresponse measurement was made. Finally, the sample was turned over so that the thick, opaque electrode was illuminated, consequently blocking the incident light from the sample. Photoresponse measurements were made once again for both polarities of applied potential.

If the observed photoresponse is due to photoconductivity, with carrier generation occurring uniformly throughout the sample, the dc photoresponse of the sample will be independent of the polarity of the applied potential. The condition of uniform carrier generation will be satisfied whenever the sample is nearly transparent in the photon energy range of interest. Whether this was the case was verified by transmission spectroscopy measurements. The magnitude of the photoresponse will also depend strongly on the orientation of the sample, being greater when the thin electrode is illuminated. If these conditions are not satisfied, then some type of photoemission is involved.

When photoemission was observed, measurements with the light incident on the opaque electrode distinguished between photoemission from surface states of the sample and from the contacts. When the sample is illuminated from the thick, opaque side, most absorbed light is absorbed by the electrode. If surface states are the source of carriers, they will be shaded by the electrode and little photoresponse will be observed. The thick, opaque electrodes are not sufficiently thick, however, to block photoemitted electrons from reaching the sample surface, and if the metal is the source of carriers, a photoresponse approximately equal in magnitude to that produced with the thin, transparent electrode illuminated will be observed.

The same procedure also determines the sign of photoemitted majority carriers. Consider a sample with the thick, opaque electrode illuminated and at positive potential. Under these conditions, only carriers of positive sign (holes) will be injected from the thick, opaque electrode into the sample, contributing to the measured photoresponse. Similarly, only carriers of negative sign (electrons) are injected with the thick, opaque electrode at negative potential. The photoresponse curves will in general be different, and the sign of the charge carriers can be unambiguously determined.[8]

A slightly different analysis is necessary when carrier generation in the bulk of the material is not uniform. This commonly occurs when the sample in question is "strongly absorbing," i.e., when the optical attenuation length $\delta$, defined by the depth at which $I/I_0 = 1/e$, is small compared with the sample thickness $d$. When $\delta \ll d$, carriers are generated predominantly in a thin layer at the surface of the sample. This results in only one sign of carrier transversing the sample for a given field direction, and the photoresponse is polarity dependent as described for photoemission. However, the magnitude of the response will still be dependent on sample orientation.

In order to eliminate the effects of photoemission while making photoconductivity measurements, it is necessary to use an electrode material which is either nonphotoemissive or which has a known photoemissive response. In practice, graphite electrodes were found to make Ohmic contact to $MgAl_2O_3$, and therefore to be nonphotoemissive. Consequently, graphite contacts were used for all photoconductivity measurements where it was desirable to exclude photoemission.

### E. Calculation and data reduction

Initial photocurrent data were converted to current density and then divided by the incident photon flux per unit area to obtain $Y$ equals quantum yield divided by incident photon. This quantity was then plotted against $h\nu$ to illustrate spectral response of the photoeffect. Photoemission data were further analyzed according to the method of Fowler[9] to determine barrier heights. This involved plotting the square root of $Y$ vs $h\nu$ to obtain an energy intercept corresponding to the desired barrier height.

### F. Optical measurements

Optical spectra were measured with a Cary model 14 spectrophotometer over the range 8000–1900 Å (1.5–6.5 eV). The sensitivity and sample thicknesses allowed detection of all absorption bands absorbing greater than $5\times10^{-2}$ of the incident flux.

### G. Far-uv measurements

Measurements of photoresponse in the region 6–40 eV were made using synchrotron radiation as a light source. A McPherson grating monochromator with a range of 6000–30 Å and a resolution of ±3 Å (corresponding to an energy width of ±0.09 eV at 20 eV) directed light onto the sample.

Measurements were made by scanning from long to short wavelengths, without a shutter, while re-

cording the photocurrent. Relative measurements of flux per unit area were made with sodium salicylate and a photomultiplier so that photoresponse could be calculated in arbitrary units. All measurements were normalized to a constant synchrotron beam current. The assumption was made that both photocurrent and incident flux depend linearly on beam current.

## III. RESULTS

### A. Photoemission

Photoemission of electrons into spinel was observed from Pt, Au, Cu, Ta, and Mo. Hole emission was observed from both Pt and Au.

Figure 3 is an example of the method of Fowler[9] for Ta electrodes. The data points corresponding to photon energies greater than or equal to about 3.5 eV fit a straight line, whose intercept yields a value of 2.75 eV for the barrier height. (The points for low photon energies depart from the straight-line fit due to thermal effects.[9]) Additional measurements yielded an average value of 2.65 eV ± 0.05 eV for this material, and changing the polarity of the applied voltage as previously discussed allowed us to determine that the charge carriers were of negative sign, i.e., electrons. Figure 4 shows that for some contact materials, specifically Pt, two types of charge carrier are involved. Photoemission begins near 3 eV for electrons and near 4.5 eV for carriers of positive sign, i.e., holes. Plots such as those of Fig. 3 were used to obtain the numbers tabulated in Table I. The meanings of the Table headings are explained pictorially in Fig. 5.

With graphite contacts, as previously noted, no photoemission was detected. Furthermore, the current-voltage characteristic, measured with a guard-ring to eliminate surface conductance, was linear to within 10% over the range ±1200 V. The

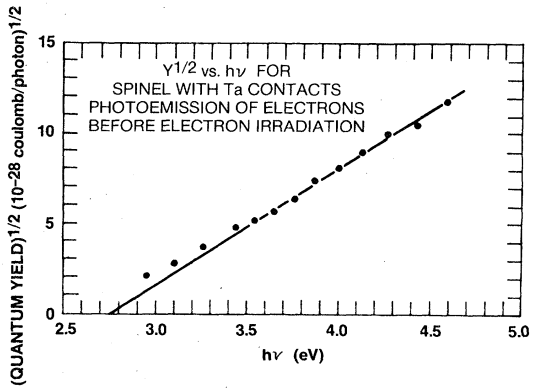


FIG. 3. A representative Fowler plot used to determine photoemissive barrier heights.

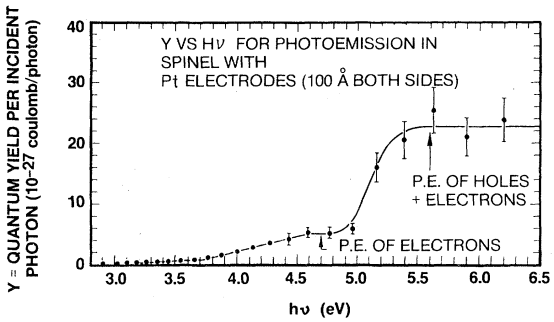


FIG. 4. Photoresponse of an unirradiated spinel sample, showing evidence of photoemission (P.E.) currents produced by both electrons and holes.

resistance obtained from the slope of the IV curve gave a bulk resistivity of $\sim 4\times 10^{16}\ \Omega$ cm. From these data, we conclude that the graphite-spinel contact is Ohmic at room temperature.

### B. Photoconductivity data

No significant response attributable to defect centers was observed in unirradiated samples. Pure crystals, iron-doped crystals, and nonstoichiometric crystals containing excess $Al_2O_3$ were carefully examined in the energy range 0.75–6.5 eV, but, with the possible exception of a weak band at 5.5 eV, all observed photoresponse resulted from photoconductivity associated with the tail of the band edge or from photoemission.

Figure 6 compares the photoconductivity produced by irradiation of spinel with 1.1-MeV gamma rays, 2.0-MeV electrons, and reactor neutrons. For gamma irradiation, six separate peaks are visible, at 3.75, 4.0, 4.25, 4.5, 5.0, and 5.5 eV. These peaks seem to be of comparable half-widths, about 0.5 eV. Electron irradiation produces the same six peaks, whereas neutron-irradiated samples show only three, apparently identical with the 4.5-, 5.0-, and 5.5-eV peaks previously described.

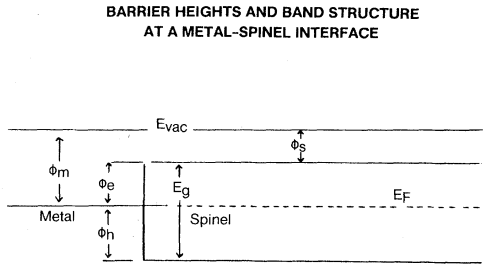


FIG. 5. Band structure at a metal-spinel interface, showing energy difference tabulated in Table I. The intercept of a plot such as Fig. 3 yields values of $\phi_e$ and $\phi_h$, $\phi_m = E_F$ is the surface work function of the metal of the contact; $\phi_s$ is the difference between $E_{vac}$ and the position of spinel-conduction band.

TABLE I. The positions of the magnesium aluminum spinel conduction and valence bands relative to $E_{vac}$.

| Metal (symbol) | $\phi_m$ (AIP) [c] (eV) | $\phi_e$ [a] (eV) | $\phi_h$ [b] (eV) | $\phi_s$ [b] (eV) | $E_g$ [b] (eV) |
|---|---|---|---|---|---|
| Cu | 4.47 | 2.70 | *N.O.* [d] | 1.77 | >8.5 |
| Au | 4.58 | 3.55 | 5.0 | 1.03 | 8.55 |
| Pt | 5.29 | 3.40 | 4.52 | 1.89 | 7.92 |
| Ta | 4.12 | 2.65 | *N.O.* [d] | 1.47 | >8.5 |

[a] ±0.05 eV.
[b] ±0.10 eV.
[c] From values given in the A.I.P. Handbook.
[d] Not observed; beyond range of monochromator.

Relative magnitudes of certain peaks vary from sample to sample; e.g., the 4.5-eV peak is greater than any other on the gamma-irradiated sample, whereas on the neutron-irradiated sample it is the smallest. The significance of these variations is difficult to assess.

The photoconductive response is compared with the optical absorption in Fig. 7. The solid curve labeled "neutron" irradiated was obtained from the same sample that gave rise to the middle curve of Fig. 6. The curve labeled "electron" irradiated was obtained on a sample electron irradiated to a dose comparable to that used for the sample yielding the photoconduction data of the lowest curve of Fig. 6. No curve is shown for a gamma-irradiated sample. Gamma irradiation produced very little if any measurable absorption at photon energies greater than 4 eV, although gamma irradiation or low-dose electron irradiation (~$10^{12}$ R) produced

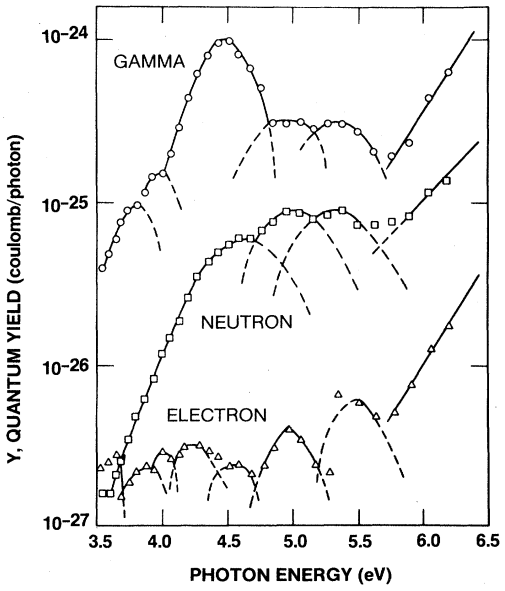


FIG. 6. Defect center photoconductivity spectrum of irradiated spinel samples.

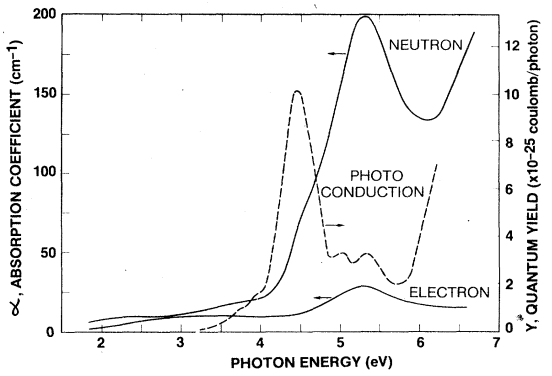


FIG. 7. Illustration of photoconductivity versus optical absorption spectrum for various irradiated spinel samples. The response is given in terms of current per relative incident photon flux as determined by a sodium salicylate detector.

some absorption between 2–4 eV, and reduced the $Fe^{3+}$ charge-transfer bands at 4.8 and 6.4 eV.[10]

The dashed line shown in Fig. 7 is the photoconductivity spectrum of the gamma-irradiated sample shown in Fig. 6. It is clear that the main absorption band at 5.3 eV produced by heavy irradiation, does not correspond to any of the photoconductivity peaks. In fact the data show no correlation whatever between the radiation-induced photoconductivity and optical absorption. Electron and gamma irradiation also resulted in increased dark current and increased photoemission current from metal contacts. Increases in the maximum value of $Y$, up to 4 orders of magnitude (to $10^{-23}$ C/incident photon), were observed.

Figure 8 gives results of intrinsic, rather than defect center, photoconductivity in unirradiated magnesium aluminum spinel. In the far-ultraviolet the quantum yield $Y$ increased rapidly with photon energy in the energy range 7–9 eV; a shoulder was observed at $h\nu \cong 11$ eV and a maximum at $h\nu \cong 15$ eV. During the course of these measurements an interesting anomaly was noted. Samples with Au electrodes produced a second maximum at $h\nu \cong 30$ eV.

### C. Other data

Time-dependent effects were observed in both virgin and irradiated samples. In virgin samples these effects were small, of the order of a few percent of the total response. The photoresponse (both photoemission and photoconductivity) decreased upon exposure to uv light. Dark resting for 24 h was sufficient to restore the original photoresponse. In irradiated samples, this effect was larger. The photoresponse decreased 5 to 20% upon successive measurements at the same wavelength. There was also a decay of

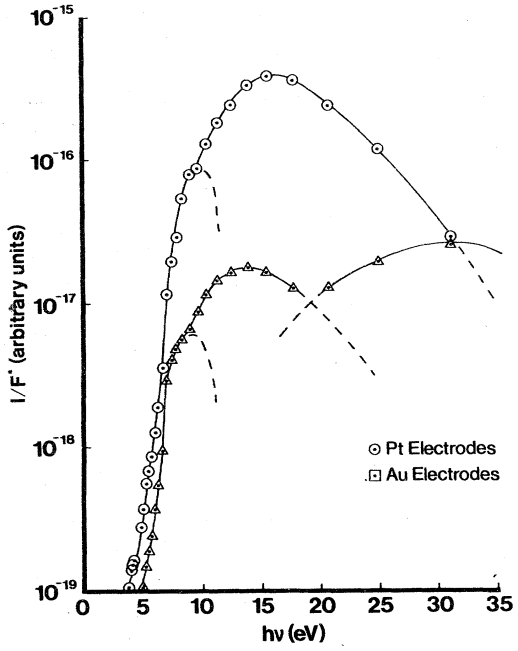


FIG. 8. Intrinsic photoconductivity spectrum of pure spinel, in the vacuum-uv energy range.

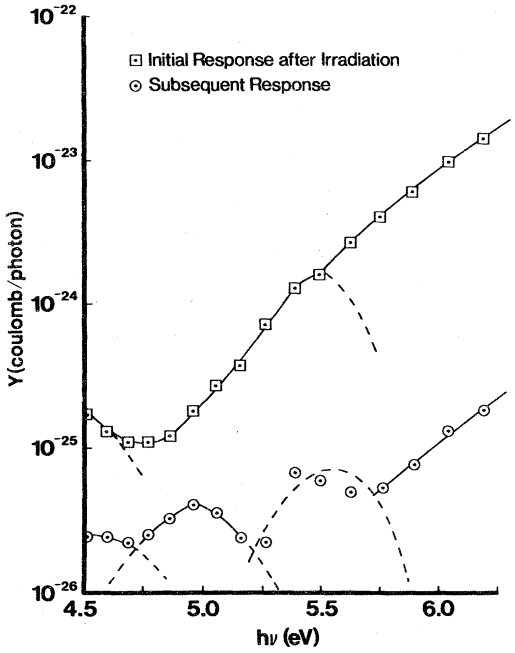


FIG. 9. Transient versus steady-state photoconductivity spectrum of an electron-irradiated spinel sample.

photoresponse in the dark which could be reinduced only by further irradiation. The decay rate was difficult to determine because of the concurrent uv bleaching during each measurement.

In electron-irradiated crystals, a large transient photoconductivity near the cutoff point of the monochromator (>6 eV) was observed. After illumination with uv light in the course of making the initial measurement, this transient response disappeared (see Fig. 9) and the photoconductivity as represented by the curve for the second run reappeared. This curve is similar to the "electron" curve of Fig. 6, although the magnitude of $Y$ differs. The transient could be reinduced only by further gamma or electron irradiation.

## IV. DISCUSSION

### A. Photoemission

According to Fowler's theory[9] of photoemission of electrons into vacuum from a metal, the quantum yield $Y$ is proportional to the quantity $(h\nu - h\nu_0)^2$, where $h\nu_0$, the threshold energy, is the difference in energy between the Fermi level of the metal and the vacuum energy level (Fig. 3). When $Y^{1/2}$ is plotted vs $h\nu$, the intercept on the energy axis is $E = h\nu_0$. Owing to thermal effects, the relationship $Y \propto (h\nu - h\nu_0)^2$ does not hold as $h\nu \to h\nu_0$, and the intercept is determined from those data points which fit a linear relationship. In the present case, where emission is into either the valence or conduction band of the magnesium aluminum spinel, such a plot determines the electron barrier ($\phi_e$), i.e., the difference in energy between the Fermi level of the metal and the bottom of the spinel conduction band. When the carriers are holes, the threshold value determines the hole barrier ($\phi_h$), i.e., the difference in energy between $E_f$ and the top of the spinel valence band. It is assumed that the optical constants of the electrode-insulator system do not change significantly over the energy range measured. This assumption is justified, since the optical constants of metals are weakly energy dependent and our optical work, as well as that of Stein,[11] shows that the same is true for pure spinel in the energy range 2 to 6 eV.

When electrons and holes are emitted from the same electrode material, this threshold energy data can be combined to construct a self-consistent energy-band diagram for the metal-spinel interface.[12] Since band bending can usually be neglected in a wide band-gap insulator, the band gap of the spinel, $E_g$, is simply $\phi_e + \phi_h$. In addition, knowledge of the position of the metal's Fermi level relative to the vacuum level ($E_{vac}$) enabled us to locate the positions of the magnesium aluminum spinel conduction and valence bands relative to $E_{vac}$. These are the values summarized in Table I.

### B. Photoconductivity

Studies of radiation-induced defect center photoconductivity have established a lower limit for the

charge carrier range/unit field, i.e., $\mu\tau$ product, in electron-irradiated spinel. Only a lower-limit estimate is possible in the absence of quantitative data relating optical absorption to photoconductive transitions.

Let us assume that all photoconductivity-producing photons are absorbed by a single defect and generate free carriers which give rise to the observed response. Then, from theory,[5]

$$J_{pc} d^2/NeV = \lambda/E = \mu\tau, \quad (1)$$

where $J_{pc}$ is the photocurrent in A/cm$^2$, $d$ is the sample thickness, $N$ is the number of photons absorbed/sec cm$^2$, V is the applied voltage, $E$ is the electric-field intensity, $\lambda = (\mu\tau)E$ is the mean carrier displacement, $\mu$ is the conductivity mobility, and $\tau$ is the mean lifetime of a charge carrier.

From the optical spectra, any optical absorption that would correspond to photoconductivity peaks is less than $5\times10^{-2}$ of the incident photon flux. Since the incident flux is of the order of $10^{13}$ photons/sec cm$^2$, it is reasonable to assume that $N \leq 5\times10^{11}$ photons/sec cm$^2$. Maximum values of $J_{pc}$ are $10^{-10}$ A/cm$^2$ with V = 520 volts and a sample thickness of about 0.3 mm. Substituting in Eq. (1) $\mu\tau \geq 2\times10^{-9}$ cm$^2$/V.

This calculation will still be valid if the photoresponse is due to a distribution of different centers, as long as only one type of carrier is excited.[5] Equation (1) becomes

$$\frac{J_{pc} d^2}{NeV} = \frac{\lambda}{E} \sum (\eta_i f_i), \quad (2)$$

where $\eta_i$ is the probability of a photoconductive transition occurring per absorption of a photon by the $i$th type of center and $f_i$ is the fraction of the total absorbed photon flux which is absorbed by centers of this type. We sum over all defects to calculate the total response, which means that $\sum_i \eta_i f_i = 1$, and Eq. (1) results.

The value of $\mu\tau$ ($2\times10^{-9}$ cm$^2$/V) is similar to that reported[5] for similar high-resistivity materials. In addition, the observed change in maximum $J_{pc}$ (as well as dark current) with time in a given sample under the same conditions suggests that the $\mu\tau$ product changes, depending on the sample radiation history. This change can be explained by the use of a model involving a distribution of traps. In unirradiated samples, the traps are empty and $\tau$ is very short. The conductivity is very low because any free carriers generated are trapped almost immediately. During irradiation, carriers are exited out of the valence band, and significantly populate the traps. Because the traps are nearly full, $\tau$ is greatly increased and both dark and photocurrents increase by orders of magnitude. This increased conductivity slowly decays as first the shallow and then the deeper traps are emptied by thermal excitation. Because the increase in dark conductivity is approximately 4 orders of magnitude, and $J_{pc} \propto \mu\tau$ with $\mu$ expected to be constant, the $\mu\tau$ product of the unirradiated sample is probably about 4 orders of magnitude lower, i.e., around $10^{-12}$ or $10^{-13}$ cm$^2$/V.

One of the unexplained puzzles of this research is the identity of the center of centers responsible for the triple peak observed at 4.5, 5, and 5.5 eV. The fact that there are no corresponding optical absorption bands indicates that the concentrations involved are low. Three peaks, equally spaced in energy and of the same half-width, could mean that three excited states of the same center rather than three separate centers are involved. The absorption band shown in Fig. 6 is in the range where $F$ and $F^+$ center absorption might be expected by analogy with MgO and $Al_2O_3$ (Refs. 5, 9, and 13). This band increases monotonically with irradiating particle momentum and fluence, whereas the photoconductivity does not. Thus we conclude that the photoconductivity we have observed is not related to $F$-type centers. Since relatively light gamma irradiation produces a photoconductivity spectrum similar to that produced by heavier-particle irradiation, we feel that the photoconductivity in all these irradiated samples is probably due to impurity or defect species produced or populated by simple ionization.

Results of the vacuum-uv measurements[14] confirm the model of the spinel electronic structure derived from photoemission measurement. The increase in conductivity between 6 and 8 eV is consistent with that expected for production of excitons as reported for $Al_2O_3$.[14] We explain the features of the photoresponse at energies $\geq$8 eV as follows: Band to band transitions begin between 8 and 9 eV, and at energies $\geq$11 eV, photoemission from the top of the valence band begins. (The energy difference between the bottom of the conduction band and the vacuum level is 2 eV, and the band gap is 9 eV.) Above 15 eV, the photoresponse begins to decrease, and above 20 eV falls sharply. A similar result of the declining photoresponse with increasing photon energy in $Al_2O_3$ has been interpreted as being due to the incident photon energy exceeding the difference between the bottom of the valence band and the vacuum level.[15] Consistent with this explanation, and given that the energy difference from the top of the valence band to the vacuum level is ~11 eV, we conclude that the valence band of spinel is ca. 8 to 9 eV wide.

The peak at $h\nu \simeq 30$ eV that is associated with Au electrodes remains unexplained. Published photo-

emission data for Au (Ref. 16) report no peak in this energy range.

## V. CONCLUSIONS

From photoemission and vacuum-uv photoconductivity data, we have constructed a self-consistent energy-band diagram for the metal-spinel interface.

The lifetime of free carriers in spinel is small in unirradiated samples, and is increased by several orders of magnitude through irradiation. The lifetime is controlled by trapping of charge carriers rather than recombination of electron-hole pairs. Both electron and hole currents have been observed.

Defect center photoconductivity in spinel may not be associated with the *F* center as reported for MgO, and the fact that photoemission of holes from platinum electrodes occurs in the same energy range (5 to 6 eV) makes it desirable to re-examine all MgO data.

The large number of peaks observed in measurements on irradiated samples indicate that at least two and possibly as many as six different centers may be contributing to the photoconductive response. Impurities such as Fe, and deviations from stoichiometry, do not produce photoconductivity and hence the photoconductivity is not due to defects associated with either of these sources. The photoconductive response produced by irradiation is not permanent, but slowly decays or anneals at room temperature, suggesting that the observed photoconductivity is associated with simple ionization.

## ACKNOWLEDGMENTS

This research was sponsored by the Division of Materials Science, U. S. Department of Energy under Contract No. W-7405-eng-26 with the Union Carbide Corporation.

[1]J. H. Schulman and W. D. Comption, *Color Centers in Solids* (Macmillan, New York, 1962), Chap. III.
[2]N. F. Mott and R. W. Gurney, *Electronic Properties in Ionic Crystals* (Oxford University Press, London, 1940), Chap IV.
[3]R. S. Crandall and M. Mikkor, Phys. Rev. 138, 1247 (1965).
[4]W. T. Peria, Phys. Rev. 112, 423 (1958).
[5]R. W. Roberts and J. H. Crawford, Jr., J. Nonmetals 2, 133 (1974).
[6]M. A. Gilleo, Phys. Rev. 91, 534 (1953).
[7]A. M. Goodman, Phys. Rev. 144, 588 (1966).
[8]Richard Williams and Richard H. Bube, J. Appl. Phys. 31, 968 (1960).
[9]R. H. Fowler, Phys. Rev. 38, 45 (1931).
[10]G. S. White, K. H. Lee, and J. H. Crawford, Jr., Phys. Status Solidi A 42, K137 (1977).
[11]H. J. Stein, Solid-State Electron. 15, 1209 (1972).
[12]R. Williams, in *Semiconductors and Semimetals*, edited by A. C. Beer and R. K. Willardson (Academic, New York, 1970), Chap. 11.
[13]K. H. Lee and J. H. Crawford, Jr., Phys. Rev. B 15, 4065 (1977).
[14]These measurements were performed at the Synchroton Radiation Center, University of Wisconsin, Madison. The authors wish to acknowledge the valuable assistance of Dr. Roger Otte.
[15]E. R. Ll'mas and A. I. Kuzonetsov, Fiz. Tverd. Tela (Leningrad) 14, 1464 (1972) [Sov. Phys.—Solid State 14, 1255 (1972)].
[16]I. Lindau, P. Pianetta, K. Y. Yu, and W. E. Spicer, Phys. Rev. B 13, 492 (1972).